INTERNATIONAL JOURNAL FOR NUMERICAL METHODS IN FLUIDS, VOL. 2, 123–149 (1982)

GENERAL CONSIDERATIONS OF NUMERICAL STABILITY AND ACCURACY IN INVISCID, COMPRESSIBLE FLOW CALCULATIONS EMPLOYING PRIMITIVE VARIABLES

C. BOSMAN,* D. AHRABIAN† AND M. KAHROM†

The University of Manchester Institute of Science and Technology, P.O. Box 88, Sackville Street, Manchester M60 1QD, U.K.

SUMMARY

The numerical stability of a number of computation schemes currently used for three-dimensional, inviscid, compressible flow is analysed using one-dimensional Fourier analysis. Whereas Reference 1 analysed schemes which were modified to render them amenable to simple analysis, the present work analyses the stability of schemes as actually used by Highton,[3] Ahrabian,[1] Denton[2] and Spalding.[6] The use of current values of the variables as they become available is shown to bring a general improvement to stability margin. The manner of damping introduced by the time marching formulation is shown to be deleterious to modifications which reduce truncation error. Staggered grid schemes can be formulated to second order accuracy with better stability margin than the corresponding first order scheme. While unstaggered grid schemes can be formulated to second order error and remain stable, their stability margin becomes very small. Agreement of the theory with numerical experiments continues to be of a high order for both one and three-dimensional disturbances.

KEY WORDS Three-dimensional Flow Computation Scheme Time Marching Conventional Damping Old Time Level Current Time Level Fourier Perturbation Staggered Grid

INTRODUCTION

The numerical stability of three-dimensional inviscid compressible flow calculations by application of one-dimensional Fourier analysis of the perturbed equations about the point of solution was examined in Reference 1. The analyses there contained were confined to the type of scheme used by Ahrabian,[1] Denton,[2] Highton[3] and Al-Nakeeb[4] which are formulated on a time marching basis. These analyses were further confined to these schemes when only previous time level values are used on the right hand side (r.h.s.) of the equations because the simple quadratic equation which determines the eigenvalues governing stability, becomes a cubic when current values are introduced into the r.h.s. of the equations. It is then simpler to test the stability of the schemes experimentally with a computer program than attempt to solve the cubic equation. The value of Reference 1 lay in exposing the basic mechanism through which the different discretization schemes operate to stabilize or destabilize the calculation. In these simple cases it was possible to see how the experimentally well established upwind and downwind biasing of differencing schemes, as had been observed by March and Merryweather,[5] were able to produce stability, at least for isentropic flow. It further became clear how a staggered grid system as used by Highton[3] was able to

*Lecturer, Mech. Eng., U.M.I.S.T.
†Postgraduate students, Mech. Eng., U.M.I.S.T.

0271-2091/82/020123-27$02.70

Received 5 November 1980
Revised 21 September 1981

combine improved accuracy in some of the terms without loss of stability. For all the schemes analysed it became apparent that stability decreased and finally vanished as the Mach number was reduced to zero. The numerical experiments which accompanied the analyses demonstrated not only the reliability of the one-dimensional stability analysis to predict stability margins for one-dimensional flows with plane disturbances but further demonstrated the coincidence of this stability margin with that obtained from three-dimensional disturbances in one-dimensional flows. It was this latter feature which encouraged the present persuit of more extensive developments and investigations.

It is usual practice to use current values of the variables on the r.h.s. of the equations as they became available. It is observed experimentally that for time marching schemes this feature modifies the low Mach number behaviour so that instead of stability vanishing as $M \rightarrow 0$, the stability margin approaches its maximum value of unity and the margin is generally improved throughout the flow range. In the present paper it is shown that the solution of the cubic stability equation reflects this characteristic and that unlike the previous analyses[1] the lower bound of the stability margin is not necessarily dictated by the low frequency perturbations. The theoretical lower bound of stability margin continues to predict reliably the experimental behaviour. The time marching formulation of the equations is here considered natural in the sense that their form arises from the natural, physical time dependent equations. In the discretized equations the damping occurs through the imposition of an arbitrarily selected time step so that the damping factor Q, which is in this case the Courant number, occurs in the equations an an inherent part of the formulation. It is shown that the occurrence of damping in this manner is deleterious to the stability of discretized forms aimed at achieving higher accuracy and that superior behaviour is achieved by introducing the damping alternatively through an additional equation in the conventional manner.

Alternative forms of the discretized equations obtained by removing arbitrarily selected terms to the left hand side (l.h.s.), as by Spalding,[6] are here regarded as unnatural because of the arbitrariness of this procedure. Such formulations involve the division of the r.h.s. by arbitrary factors involving fluid properties which have pronounced effects on stability. The Spalding formulation is studied in the present work and found to possess inferior low Mach number stability margin and limited subsonic range.

Spalding's scheme employs an auxiliary correction cycle as an innate part of the total composite cycle. Highton's scheme contains a similar device as an option but such devices may be introduced into any scheme to form a composite cycle. The present work analyses a generalized auxiliary cycle and applies the results to Highton's scheme where the effect on the composite cycle is also considered. A considerable improvement in stability results as would be anticipated since the axiliary equations are usually chosen with a very high stability margin. Spalding's auxiliary implementation, based on a diffusive pressure correction concept is quite different from Highton's and poses severe analytical difficulties. However his auxiliary equations, implemented in the manner of Highton, have been analysed and show a similar level of improvement to the stability margin of the composite cycle.

It should be observed that the basic schemes of Ahrabian[1] and Denton[2] coincide when applied to the one-dimensional flows here treated.

GENERAL STABILITY CONSIDERATIONS

Let the non-linear algebraic difference equations for compressible flow

$$\bar{E} = 0 \tag{1}$$

to be solved for the primitive variables $\bar{x}$, be written in the form of the recurrence relation

$$\bar{x}^{n+1} = \bar{x}^n - \bar{E}^{n,n+1} \tag{2}$$

where $\bar{E}$ is indicated as containing the variables $\bar{x}$ at the new and old level values, $(n+1)$ and (n) respectively. The recurrence relation (2) may not be found to be stable on being repeatedly cycled. Stability may often be achieved by the introduction of a damping (or relaxation) factor Q which may be introduced in one of the following two ways

$$\bar{x}^{n+1} = \bar{x}^n - Q\bar{E}^{n,n+1} \tag{3}$$

or

$$\bar{x}^{n+1} = \bar{x}^n - \bar{E}^{n,n+1} \tag{4a}$$

$$\bar{x}^{n+1} := \bar{x}^n + Q(\bar{x}^{n+1} - \bar{x}^n) \tag{4b}$$

Although substitution of (4a) into (4b) causes the result to look identical to (3), this is not necessarily so as the following simple linear example demonstrates.

Let the variables be $\bar{x} \equiv \begin{bmatrix} x_1 \\ x_2 \end{bmatrix}$ and the equations $\bar{E}^{n,n+1} = 0$, be

$$ax_1^n + bx_2^n = 0 \tag{5a}$$

$$cx_1^{n+1} + dx_2^n = 0 \tag{5b}$$

then from (3)

$$x_2^{n+1} = x_1^n + Q(e(x_1^n - Q(ax_1^n + bx_2^n)) + dx_2^n) \tag{6}$$

is obtained, whereas from (4a) and (4b)

$$x_2^{n+1} = x_1^n + Q(c(x_1^n - (ax_1^n + bx_2^n)) + dx_2^n) \tag{7}$$

is obtained. If on the other hand $\bar{E} = \bar{E}^n$, containing only the old level values (n), then (4a) with (4b) becomes the same recurrence relationship as (3). The distinction is important because both forms (3) and (4) occur in natural formulations of the compressible flow equations and their respective stability behaviours are quite different in a profound way, as will be seen subsequently.

In considering the solution of the steady state compressible flow equations represented by (1), the form (3) naturally occurs if the time dependent flow equations are used, as discussed by Bosman and Ahrabian,[1] as a vehicle to arrive at the steady state in which case the damping factor Q becomes the Courant number defined by

$$Q \equiv \frac{c\Delta t}{\Delta z} \tag{8}$$

and can be seen to have physical significance. Alternatively the steady state equations may be written as in (4a), in which case the damping factor Q in (4b) has no physical significance.

We consider the linear stability of the relations (3) and (4) about the point of solution $\bar{x}_s$ which satisfies (1), then from (3)

$$(\bar{x}^{n+1} - \bar{x}_s) = (\bar{x}^n - \bar{x}_s) - Q(\bar{E}^{n,n+1} - \bar{E}) \tag{9}$$

so that by Taylor expansion about $\bar{x}_s$

$$\delta\bar{x}^{n+1} = \delta\bar{x}^n - Q(G_n\delta\bar{x}^n + G_{n+1}\delta\bar{x}^{n+1}) \tag{10}$$

which by re-arrangement gives

$$\delta\bar{x}^{n+1} = (I + QG_{n+1})^{-1}(I - QG_n)\delta\bar{x}^n \tag{11a}$$

or starting with (4) we obtain instead

$$\delta\bar{x}^{n+1} = (I + G_{n+1})^{-1}(I - QG_n)\delta\bar{x}^n \tag{11b}$$

where

$$\delta\bar{x}^n \equiv \bar{x}^n - \bar{x}_s \tag{12}$$

$$G_{n;i,l} \equiv \left[\frac{\partial E_i^{n,n+1}}{\partial x_l^n}\right], \qquad G_{n+1;i,l} \equiv \left[\frac{\partial E_i^{n,n+1}}{\partial x_l^{n+1}}\right]. \tag{13}$$

The difference in the perturbation equations (11a) and (11b) is apparent when $G_{n+1} \neq 0$ and follows the earlier discussion leading to (6) and (7).

As discussed by Bosman and Ahrabian[1] the perturbation vectors $\delta\bar{x}$ contain values at points around and including the nodal point p. By Fourier series we may express the values at any point j in terms of the value at the nodal point p and an arbitrary frequency parameter ω such that

$$\delta x_j = \sum_{\omega} (e^{i\omega(j-p)} + e^{-i\omega(j-p)})\delta x_p \tag{14}$$

Since the two terms in the bracket are conjugate, their growth or decay behaviour is similar and we need examine the stability of only the one with the positive index sign, i.e. $e^{i\omega(j-p)}$. Since the algebraic equations (1) are formulated from differential equations all of whose terms contain derivatives then all terms in the algebraic equations (1) contain differences of values of x about the nodal point p. Hence in the neighbourhood of the uniform perturbation represented by $\omega = 0$ a difference between two points j and m in one space dimension takes the form

$$(\delta x_j - \delta x_m) \xrightarrow[\omega\to 0]{} \frac{(e^{i\omega(j-p)} - e^{i\omega(m-p)})}{(j-m)}\bigg|_{\omega\to 0} \delta x_p$$

$$\longrightarrow \frac{i\omega(j-m) - \dfrac{\omega^2}{2}(j+m-2p)(j-m)}{(j-m)}\,\delta x_p$$

$$\longrightarrow \left(i\omega - \frac{\omega^2}{2}(j+m-2p)\right)\delta x_p \tag{15a}$$

$$\longrightarrow 0 \tag{15b}$$

If these multiples of δx_p in (15a) are absorbed into the govering matrices G of (11) or (13) then the elements of G become complex numbers multiplied by real fluid properties, e.g. Mach number (M), density (ρ), acoustic speed (c), etc. and (11) or (13) now apply to the variables, i.e. fluid properties x at the single nodal point p.

Now (11) becomes

$$\delta\bar{x}_p^{n+1} = (I + QG_{n+1})^{-1}(I - QG_n)\delta\bar{x}_p^n \tag{11a}$$

and (13) becomes

$$\delta\bar{x}_p^{n+1} = (I + G_{n+1})^{-1}(I - QG_n)\delta\bar{x}_p^n \tag{13a}$$

As $\omega \to 0$ *every* element of G contains a factor of the form

$$\left(i\omega - \frac{\omega^2}{2}(j+m-2p)\right) \to 0 \tag{16}$$

from (15a) and (15b).

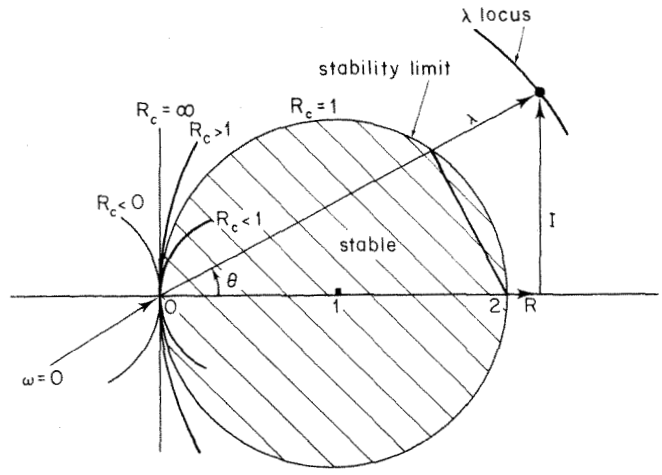

Figure 1. Argand diagram of basic stability behaviour. $Q\lambda < 2\cos\theta$, $\cos\theta = R/\sqrt{(R^2+I^2)}$, $\lambda = \sqrt{(R^3+I^2)}$, $Q \leq 2R/(R^2+I^2)$

It follows from (16) that

$$G \xrightarrow[\omega \to 0]{} [0] \tag{17}$$

hence the eigenvalues of G, λ, defined by

$$|\lambda I - G| \equiv 0 \tag{18}$$

satisfy the condition

$$(\lambda) \xrightarrow[\omega \to 0]{} 0 \tag{19}$$

and the locus of λ on the Argand diagram, (Figure 1) passes through the origin.

For negative values of ω, it can be seen from (15a) that the multipliers of δx_p conjugate and so do the values of λ_G in (18) hence the locus of λ_G is tangent to the imaginary axis at the origin. Now for stability, the λ_G must lie on or within the unit circle shown in Figure 1 so that it is necessary that the radius of curvature R_c of the λ_G locus at the origin satisfies the condition

$$0 < R_c < 1 \tag{20}$$

Now this radius of curvature is given by

$$(2R_c - \lambda_R)\lambda_R = \lambda_I^2 \tag{21}$$

where λ_R and λ_I are the real and imaginary parts of λ and at the origin $\lambda_R \to 0$, $\lambda_I \to 0$ hence

$$R_c = \left(\frac{\lambda_I^2}{2\lambda_R}\right)_{\omega \to 0} \tag{22}$$

Notice that $R_c < 0$ implies a centre of curvature on the opposite side of the imaginary axis.

Since the introduction of damping Q in the manner of (4) has the sole effect of scaling thus $\lambda := Q\lambda$ as shown by Bosman[7] then, with damping in this manner (22) becomes

$$R_c = \left(\frac{Q\lambda_I^2}{2\lambda_R}\right)_{\omega\to 0} \tag{23}$$

Although no proof of generality can be given, the authors have found that all the schemes analysed possess the common characteristic that the entire locus of a given branch of the λ locus lies to one side of the imaginary axis so that if all the branches lie on the same side of this axis, then all branches can be brought within the unit circle by the application of some suitable value of Q in the manner of (4). If the above characteristic can be assumed, then the stabilization of the numerical scheme by application of Q in the manner of (4) is assured for some values of Q satisfying

$$0 < Q < \left(\frac{2\lambda_R}{\lambda_I^2}\right)_{\omega\to 0} \tag{24}$$

It was found by Bosman and Ahrabian[1] who analysed only schemes for which $G_{n+1} = 0$, i.e.

$$\bar{E} = \bar{E}^n \tag{25}$$

where only old level values are used in the expression of the equations, that in fact the lower bound of Q occurred at $\omega = 0$. As will be seen subsequently, when $G_{n+1} \neq 0$, as is usual in most schemes in practice, the lower bound of Q may not be given by the perturbation frequency $\omega = 0$. However it remains true that if all the branches of λ lie to the same side of the imaginary axis at the origin, where $\omega = 0$, then the scheme can be stabilized by suitably low values of Q used either in the time marching form (TM) of (3) or the form of conventional damping (CD) in (4). Such schemes are here regarded as stable. On the other hand, schemes for which R_c (equation (22)) $\to \infty$, have λ lying on the imaginary axis at the origin and the λ locus at that point is not one of simple tangency, and also schemes which possess branches lying on both sides of the imaginary axis, cannot be stabilized by the application of Q and are here regarded as inherently unstable.

For the stable schemes, stability will only be realized for values of Q which confine all the resulting λ on or within the unit circle of Figure 1. Since the effect of Q with CD is simply to scale λ then in this case geometry requires that

$$Q \leqslant \frac{2\lambda_R}{\lambda_R^2 + \lambda_I^2} \tag{26}$$

The stability margin referred to in subsequent sections and plotted as Q in the Figures refers to the values of Q satisfying the equality in (26) in CD cases or for TM and more generally, the values of Q which confines all resulting λ on *and* within the unit circle.

EFFECTS OF DIFFERENCING SCHEMES

The effect of taking a difference of perturbed values of x at two grid points j and m in one space dimension is given by (15a). The direction of flow is assumed to be from m to j hence $j > m$. Equation (15a) may be re-written

$$(\delta x_j - \delta x_m) \xrightarrow[\omega\to 0]{} i\omega - \omega^2\alpha \tag{27}$$

where

$$\alpha = \frac{(j-p)+(m-p)}{2} \tag{28}$$

gives the position of the centre point about which the difference is taken, relative to the nodal point p, i.e. with p taken as local origin.

If j and m are centred on p then α vanishes. If, on the other hand, the difference is centred upwind of p then

$$\alpha < 0 \tag{29a}$$

whereas if it is centred downwind of p

$$\alpha > 0 \tag{29b}$$

the upwind and downwind differencing are of first order truncation error, whereas the centred differencing is of second order error.

It is possible to introduce improved accuracy of the differencing by extrapolating values by application of, say, a polynomial fit. As $\omega \to 0$, the perturbation Fourier component

$$e^{i\omega(s-j)} \to 1 + i\omega(s-j) \tag{30}$$

becomes linear so that all polynomials of the first or higher degree become exact fits and the extrapolated value at point s relative to point j is given by (30) in all cases. If this extrapolation is used similarly at the differencing points j and m then (27) becomes

$$(1 + i\omega(s-j))(i\omega - \omega^2\alpha) \to i\omega - \omega^2\beta \tag{31a}$$

where

$$\beta \equiv \alpha + (s-j) \tag{31b}$$

The effect (31b) is simply to shift the apparent centre point α of the difference scheme by the extrapolation distance $(s-j)$. Hence if upwind differencing is improved by forward extrapolation $(s-j)$ so that the shifted centre given by (31b) now lies at the nodal point p then $\beta = 0$ and the term in ω^2 in (31a) vanishes just as for two point central differencing, when α vanishes. All second order error differencing schemes, whether apparently biased upwind, downwind or not, cause the real part of the differencing operator to vanish as $\omega \to 0$, i.e.

$$R_a = R_b = R_c = R_d = 0 \tag{32}$$

(see (40) and (50)). This fact has important repercussions with regard to stability as will be seen subsequently.

USE OF CURRENT VALUES

If only old level values are used in $\bar{E}$ then the matrix G_{n+1} in the perturbed equations (11a) and (13a) vanishes and the effect of damping Q, in either formulation (3) or (4) is the same and has the effect of scaling λ. If we now consider the behaviour in the neighbourhood of $\omega = 0$ then

$$G_n \to [0], \qquad G_{n+1} \to [0] \tag{33}$$

and

$$(I + QG_{n+1})^{-1} \to (I - QG_{n+1}) \tag{34}$$

hence (11a) becomes

$$\delta\bar{x}_p^{n+1} = (I - Q(G - QG_{n+1}G_n))\delta\bar{x}_p^n \tag{35}$$

whereas (13a) becomes

$$\delta\bar{x}_p^{n+1} = (I - Q(G - G_{n+1}G_n))\delta\bar{x}_p^n \tag{36}$$

where

$$G \equiv G_n + G_{n+1} \tag{37}$$

Since in the neighbourhood of $\omega = 0$ all elements of G contain a factor of the type

$$i\omega + \gamma\omega^2 \tag{38}$$

as a result of the differencing procedure then the product $G_{n+1}G_n$ contains only real elements of order ω^2 and is scaled by $i^2 = -1$, lower orders, i.e. higher degrees, in ω vanishing as $\omega \to 0$.

If we consider the case of homentropic, isentropic uniform flow in one space dimension which reduces to only two variables, as was done by Bosman and Ahrabian[1] then

$$\delta\bar{x} = \begin{bmatrix} \delta V \\ \delta\rho \end{bmatrix} \quad \text{or} \quad \begin{bmatrix} \delta\rho \\ \delta V \end{bmatrix} \tag{39}$$

and if the governing matrix G is written

$$G \equiv \begin{bmatrix} a & b \\ c & d \end{bmatrix} \tag{40}$$

the use of current values as they become available implies from (37) and (10) that

$$G_{n+1} = \begin{bmatrix} 0 & 0 \\ c & 0 \end{bmatrix}, \qquad G_n = \begin{bmatrix} a & b \\ 0 & d \end{bmatrix} \tag{41}$$

and in this case

$$(I + G_{n+1})^{-1} = \begin{bmatrix} 1 & 0 \\ -c & 1 \end{bmatrix} = I - \begin{bmatrix} 0 & 0 \\ c & 0 \end{bmatrix} = I - G_{n+1} \tag{42}$$

so that (13) becomes

$$\begin{aligned} \delta\bar{x}^{n+1} &= (I - (G_{n+1} + G_n - G_{n+1}G_n))\delta\bar{x}^n \\ &= (I - (G - G_{n+1}G_n))\delta\bar{x}^n \end{aligned} \tag{43}$$

If damping as in (4b) is now applied (43) becomes

$$\delta\bar{x}^{n+1} = (I - Q(G - G_{n+1}G_n))\delta\bar{x}^n \tag{44}$$

If on the other hand, the time marching scheme as in (3) is employed then it will be seen from (11) that

$$\delta\bar{x}^{n+1} = (I - Q(G - QG_{n+1}G_n))\delta\bar{x}^n \tag{45}$$

From (41), the term $G_{n+1}G_n$ is given by

$$G_{n+1}G_n = \begin{bmatrix} o & 0 \\ ac & bc \end{bmatrix} \equiv \begin{bmatrix} 0 & 0 \\ h & g \end{bmatrix}. \tag{46}$$

The eigenvalues λ of the matrix $(G - G_{n+1}G_n)$ satisfy the equation

$$\lambda^2 - (a + d - g)\lambda + ad - bc = 0 \tag{47}$$

where it can be seen that the only effect of the use of current values is to introduce the term

$$g = bc \tag{48}$$

If one follows a similar argument with regard to the TM form of the equations then, as will be seen by comparison of (12) with (13), (14) and (15), the difference is to scale the factor g by the factor Q. From (15) we obtain the general result

$$\lambda = \tfrac{1}{2}\{a + d - Q'g \pm [(a + d)^2 - 4ad + 4Q'g - 2Q'g(a + d) + Q'g^2]^{1/2}\} \tag{49a}$$

where

$$Q' = \left\{ \begin{matrix} 0, & \text{for old level (OL) values only when } G_{n+1} = 0 \\ 1, & \text{for current values with conventional damping (CD)} \\ Q, & \text{for current values with time marching (TM)} \end{matrix} \right\} \tag{49b}$$

Recalling the earlier remarks of this section with regard to (38), let the terms of the governing matrix be written

$$f = R_f \omega^2 + I_f \omega \mathrm{i} \tag{50}$$

where $f = a, b, c$ or d in (40) and contains fluid factors such as $M, c/\rho, \rho/c$ as well as numerical coefficients. then in the neighbourhood of the origin as $\omega \to 0$

$$\lambda_R = \omega^2 (\lambda_{R_n} + Q' \lambda_{R_{n+1}}) \tag{51}$$

where

$$\lambda_{R_n} \equiv \frac{1}{2}\left(R_a + R_d \pm \frac{(R_a - R_d)(I_a - I_d) + 2(R_b I_c + R_c I_b)}{sqrt} \right) \tag{52}$$

$$\lambda_{R_{n+1}} \equiv \tfrac{1}{2} I_b I_c \left(1 \pm \frac{I_a + I_d}{sqrt} \right) \tag{53}$$

$$sqrt \equiv |((I_a - I_d)^2 + 4 I_b I_c)^{1/2}| \tag{54}$$

and

$$\lambda_I = \omega \lambda_{I_n}$$

where

$$\lambda_{I_n} = \tfrac{1}{2}(I_a + I_d \pm sqrt) \tag{55}$$

By (23)

$$R_c = \frac{Q \lambda_{I_n}^2}{2(\lambda_{R_n} + Q' \lambda_{R_{n+1}})} \tag{56}$$

where it can be seen from (49b) that for old level values and current values with CD, R_c is simply scaled by Q but not for current values with TM. The general beneficial effect of using current values can be seen from (56) and (53) where it should be observed[1] that for stability in subsonic flow b and c should be conjugate negative so that $I_b I_c > 0$ and $\lambda_{R_{n+1}}$ is usually positive.

In schemes which attempt to obtain higher accuracy the condition (32) applies with the result $\lambda_{R_n} = 0$ (see (52)) and $R_c \to \infty$ for OL schemes, with consequent failure. It should be observed from (53) that $\lambda_{R_{n+1}}$, which arises as a result of using current values, is a function of only the imaginary parts of the matrix elements and does not vanish for higher accuracy schemes. However for the TM form $Q' = Q$, and R_c at (56) is then seen to be independent of the damping factor Q and since usually $R_c > 1$, such schemes fail. In contrast, with CD, $Q' = 1$, and R_c is scaled by Q and can therefore be stabilized.

The cross-winding (i.e. opposed difference schemes or staggered mesh) of terms b and c causes the term $(R_b I_c + R_c I_b)$ in (52) to vanish as then b and c are negative conjugate to each other. This improves stability by reducing the term with the dual sign in (52). This term vanishes if in addition a and d are made equal, as is possible in differential formulations of the equations,[1] when stability is assured.

USE OF AUXILIARY CYCLE

If we define the increment in the vector $\bar{x}$ by

$$\delta'\bar{x} \equiv \bar{x}^{n+1} - \bar{x}^n \tag{57}$$

then (4a) may be written

$$\delta'\bar{x}^n = -\bar{E}^{n,n+1} \tag{58}$$

which by (1) and a Taylor expansion about $\bar{x}_s$ as at (9) and (10) may be written

$$\begin{aligned}\delta'\bar{x}^n &= -(\bar{E}^{n,n+1} - \bar{E}) \\ &= -(G_n\delta\bar{x}^n + G_{n+1}\delta\bar{x}^{n+1})\end{aligned} \tag{59}$$

where $\delta\bar{x}^n$, $\delta\bar{x}^{n+1}$ are defined as at (12) so that by (1) above

$$\delta'\bar{x}^n = \delta\bar{x}^{n+1} - \delta\bar{x}^n \tag{60}$$

Equations (59) and (60) are a re-expression of the original perturbed problem in the neighbourhood of the solution $\bar{x}_s$ involving the incremental vector $\delta'\bar{x}$ and the vector perturbation from the solution $\delta\bar{x}$. We may introduce an arbitrary set of auxiliary equations $A\delta'\bar{x}$ into (58) thus

$$\delta'\bar{x} = -A\delta'\bar{x} - \bar{E}^{n,n+1} \tag{61}$$

where A may be selected to have a stability margin superior to that of $\bar{E}$. It will be observed that if $\delta'\bar{x}$ vanishes we have the original solution $\bar{E} = 0$. Subtracting this solution from (61) as at (9), applying a Taylor expansion about $\bar{x}_s$ and considering that the auxiliary equations may contain terms at both current and old level values, then (61) may be written

$$\delta'\bar{x}^{n+1} = -(A_n\delta'\bar{x}^n + A_{n+1}\delta'\bar{x}^{n+1}) - (G_n\delta\bar{x}^n + G_{n+1}\delta\bar{x}^{n+1}) \tag{62}$$

Such a scheme may be used in place of the original one (namely (58)) and stability behaviour may be improved by suitable choice of A.

Alternatively it is possible by solving a subset

$$\bar{E}' = 0 \tag{63}$$

of the original equations $\bar{E}$, to introduce an auxiliary cycle in the manner

$$\delta'\bar{x}^n = E^{n,n+1} \tag{64a}$$

being the main cycle, and

$$\delta'\bar{x}^{n+r} = -(A_r\delta'\bar{x}^{n+r} + A_{r-1}\delta'\bar{x}^{n+r-1}) - \bar{E}'^{n,n+1} \tag{64b}$$

being the auxiliary cycle, in which, for the first pass ($r = 1$) only

$$\delta'\bar{x}^{n+r-1} = \delta'\bar{x}^n = 0 \tag{64c}$$

on the r.h.s. so that

$$\delta'\bar{x}^{n+1} = -\bar{E}'^{n,n+1} \tag{64d}$$

is the current residue of the subset $\bar{E}'$ of the principal equations.

The perturbation of these equations, following the earlier procedure, leads to

$$\delta'\bar{x}^n = -(G_n\delta\bar{x}^n + G_{n+1}\delta\bar{x}^{n+1}) \tag{65a}$$

$$\delta'\bar{x}^{n+r} = -(A_{r-1}\delta'\bar{x}^{n+r-1} + A_r\delta'\bar{x}^{n+r}) - (G'_n\delta\bar{x}^{n+r} + G'_{n+1}\delta\bar{x}^{n+r+1}) \tag{65b}$$

whereas by (60)

$$\delta'\bar{x}^{n+r} = \delta\bar{x}^{n+r+1} - \delta\bar{x}^{n+r} \tag{65c}$$

The stability of the auxiliary cycle, alone, expressed by (65b) and (65c) may be re-written

$$\begin{bmatrix} I+A_r & G'_{n+1} \\ I & -I \end{bmatrix} \begin{bmatrix} \delta'\bar{x}^{n+r} \\ \delta\bar{x}^{n+r+1} \end{bmatrix} = - \begin{bmatrix} A_{r-1} & G'_n \\ 0 & I \end{bmatrix} \begin{bmatrix} \delta'\bar{x}^{n+r-1} \\ \delta\bar{x}^{n+r} \end{bmatrix} \tag{66}$$

Even for simple isentropic, one-dimensional flow where

$$\delta\bar{x} = \begin{bmatrix} \delta V \\ \delta\rho \end{bmatrix} \tag{67}$$

this becomes a 4×4 matrix eigenvalue problem and is not amenable to simplified theoretical treatment as the 2×2 main cycle alone is.

The above development follows the typical general application of auxiliary cycles as actually implemented. Details of implementation may differ considerably in the choice of forms for A and $\bar{E}'$. In the Highton[8] auxiliary cycle for instance the auxiliary equations A consist of the equation of motion with the momentum flux term omitted and the continuity equation, while the subset of principal equations $\bar{E}'$ is null. The Spalding[6] implementation is quite different in that there, A consists of the momentum equation with the momentum flux term omitted with a diffusion expression for density correction in continuity and the subset $\bar{E}'$ consists of the continuity equation alone.

Some feel for the behaviour of these modified schemes using an auxiliary equation can be obtained by examining the Highton type of auxiliary scheme. In this case the auxiliary cycle (64b) is simplified by the removal of the dependence of $\delta'\bar{x}$ on the current residue of the subset of equations $\bar{E}'^{n,n+1}$, because they are null so that the auxiliary cycle can be expressed by

$$\delta'\bar{x}^{n+r} = -B\delta'\bar{x}^{n+r-1} \tag{68a}$$

where

$$B \equiv (I+A_r)^{-1}A_{r-1} \tag{68b}$$

so that

$$\begin{aligned} \delta'\bar{x}^{n+1} &= -B\delta'\bar{x}^{n} \\ \delta'\bar{x}^{n+2} &= -B\delta'\bar{x}^{n+1} \\ &\cdots\cdots\cdots\cdots \\ \delta'\bar{x}^{n+r} &= -B\delta'\bar{x}^{n+r-1} \end{aligned} \tag{69}$$

and by substitution and addition, the latest vector solution

$$\bar{x} \equiv \bar{x}^{n+r+1} \tag{70}$$

is given by

$$\bar{\Sigma} \equiv \bar{x} - x^{n+1} = ((-B)+(-B)^2+\ldots+(-B)^r)\delta'\bar{x}^n \tag{71}$$

which defines $\bar{\Sigma}$ and from which

$$\bar{\Sigma} = [I-(-B)]^{-1}[-B][I-(-B)^n]\delta'\bar{x}^1 \tag{72}$$

The perturbation from the solution is now

$$\begin{aligned} \delta\bar{x} &= \bar{x}^{n+r+1} - \bar{x}_s \\ &= (\bar{x}-\bar{x}^n)+(\bar{x}^n-\bar{x}_s) = \bar{\Sigma}+\delta\bar{x}^n \end{aligned} \tag{73}$$

which by (72)

$$= (I - G_B)\delta\bar{x}^n \tag{74}$$

where G_B determines the stability of the auxiliary cycle alone and is defined from (72) as

$$G_B = [I-(-B)]^{-1}[B][I-(-B)] \tag{75}$$

Now, as $\omega \to 0$, *all* non-zero elements of the auxiliary matrix A contain difference terms and tend to vanish so that

$$[I+B]^{-1} \to I - B + B^2 \tag{76}$$

to the lowest degree in $i\omega$ and ω^2, where as discussed in the previous section B^2 will be real negative and of order ω^2. Hence for $r = 1$, $\omega \to 0$

$$G_B \to B \tag{77}$$

and for $r > 1$, $\omega \to 0$

$$G_B \to B - B^2 \tag{78}$$

For the composite cycle which includes the principal equations $\bar{E}$ plus r cycles of the auxiliary equations A, we consider an initial perturbation about the solution x_s,

$$\delta\bar{x}^0 \equiv \bar{x}^0 - \bar{x}_s \tag{79}$$

which by (59) and (60) gives

$$\delta\bar{x}^1 = \delta\bar{x}^0 - (G_n\delta\bar{x}^0 + G_{n+1}\delta\bar{x}^1) \tag{80}$$

$$\equiv \bar{x}^1 - \bar{x}_s \tag{81}$$

Now introducing the auxiliary equations from (68)

$$\delta\bar{x}^2 = -B\delta\bar{x}^1 \tag{82}$$

etc. and for r cycles

$$\delta\bar{x} = (I - G_B)\delta\bar{x}^1 \tag{83}$$

by (73), where G_B is defined by (75). By (80) and (83)

$$\delta\bar{x} = (I - G_B)(I + G_{n+1})^{-1}(I - G_n)\delta\bar{x}^0 \tag{84}$$

so that as $\omega \to 0$ and $(I + G_{n+1})^{-1} \to I - G_{n+1}$

$$= [1 - (G_B + G - G_BG - G_{n+1}G_n)]\delta\bar{x}^0 \tag{85}$$

The quadrature terms $(-G_BG)$ and $(-G_{n+1}G_n)$ are both positive real as $\omega \to 0$, as previously discussed and are likely to improve stability, the second of these is simply a result of using current values in the principal equations whereas the first is a contribution from the application of the auxiliary cycle. If the stability of the auxiliary cycle alone, expressed by G_B is high compared to that of the principal equations alone expressed by G, then the composite cycle may be anticipated to have an improved stability margin over the main cycle.

COMPARISON OF THEORETICAL AND EXPERIMENTAL RESULTS

All the results presented are for isentropic, homentropic, uniform compressible flow in one space dimension as in Reference 1 where the equations have been formulated on an integral

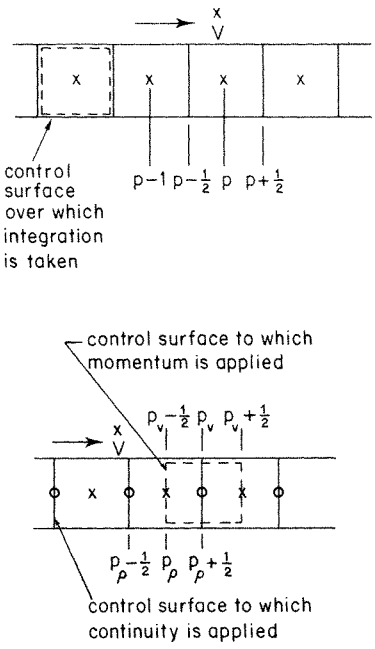

Figure 2. Illustrating the different grid systems; (a) mesh used by Denton/Ahrabian scheme; (b) Mesh used by Highton/Spalding scheme. × ρ determined at these points, ○ V determined at these points

basis as applied to fixed control surfaces and have the form

$$\bar{E}=\begin{bmatrix}(\bar{M}.\,\mathrm{grad}+\bar{M}\,\mathrm{div})\,\bar{V}+\dfrac{c}{\rho}(1+M(\bar{M}.))\,\mathrm{grad}\,\rho\\[2ex]\dfrac{\rho}{c}\,\mathrm{div}\,\bar{V}+\bar{M}.\,\mathrm{grad}\,\rho\end{bmatrix} \tag{86}$$

in which the operators div and grad have been discretized by schemes due to Highton[3,8] and Ahrabian.[1] The numerial experiments have been conducted using computer programs written for three-dimensional flow through ducts of a shape which can be arbitrarily specified by the user. One dimensional experiments have been simulated by using uniform, unidirectional flow, perturbed by plane disturbances normal to the flow. The grid employed in all cases was $3\times3\times100$ points with the plane perturbation half way along the flow at station 50, in order to avoid the influence of the stabilizing end boundaries on the results as observed in Reference 1.

The elements a, b, c, d of the governing stability matrix (40) correspond, respectively, to the perturbation of the terms $(\bar{M}.\,\mathrm{grad}+\bar{M}\,\mathrm{div})\,\bar{V}$, $\dfrac{c}{\rho}\,(\mathrm{grad}\,\rho+M\bar{M}.\,\mathrm{grad}\,\rho)$, $\dfrac{\rho}{c}\,\mathrm{div}\,\bar{V}$ and $\bar{M}.\,\mathrm{grad}\,\rho$ in (86) after suitable discretization. Figure 3 illustrates the stability margin Q against Mach number M from Ahrabian's results where the discretized equations, reduced to one dimension for analytical simplicity, read

$$\bar{E}=\frac{1}{c}\begin{bmatrix}\dfrac{1}{\rho_p}\{(\rho V^2)_p-(\rho V^2)_{p-1}+c^2(\rho_{p+1}-\rho_p)\}\\[2ex]\{(\rho V)_p-(\rho V)_{p-1}\}\end{bmatrix} \tag{87}$$

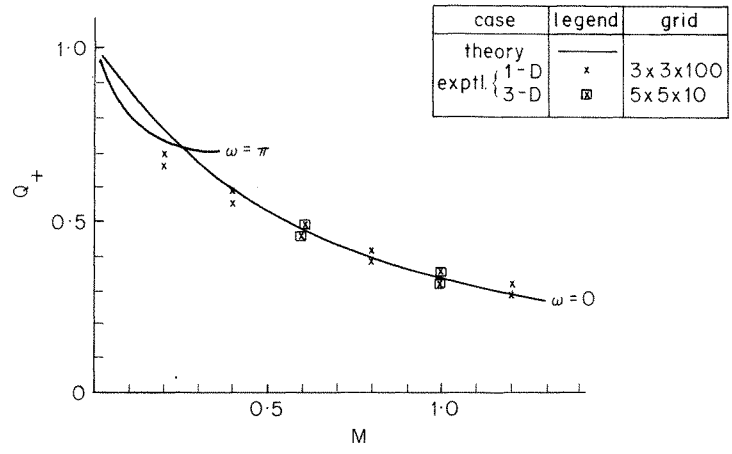

Figure 3. Stability margin Q against Mach number M with perturbation frequency ω for Ahrabian/Denton scheme with time marching using current pressure values

in which momentum and mass convection terms are upwinded while the force term $c^2(\rho_p - \rho_{p+1})$ is downwinded. This Figure shows the TM case in which the density ρ is used at its current value in the force term, which is normal practice, whereas in the momentum flux term $((\rho V^2)_p - (\rho V^2)_{p-1})$ the density is at the old level. It appears that as with schemes using only old level values[1] the lower bound of Q occurs at or close to $\omega = 0$. The stability margin compared with that obtained with old level values is greatly improved as discussed and anticipated in the section 'Use of Current Values'. Figure 4 depicts the TM case when current values of ρ are used in both the momentum flux and force terms. It will be observed that the lower bound of Q does not correspond to a particular perturbation frequency throughout the Mach number range and nowhere is it close to $\omega = 0$. Figure 5 compares the stability margins for the last mentioned case at the frequency $\omega = \pi$, when old level values are used (i.e. $Q' = 0$ in (48), when CD is used ($Q' = 1$), when $Q' = 0{\cdot}5$ and when TM is used

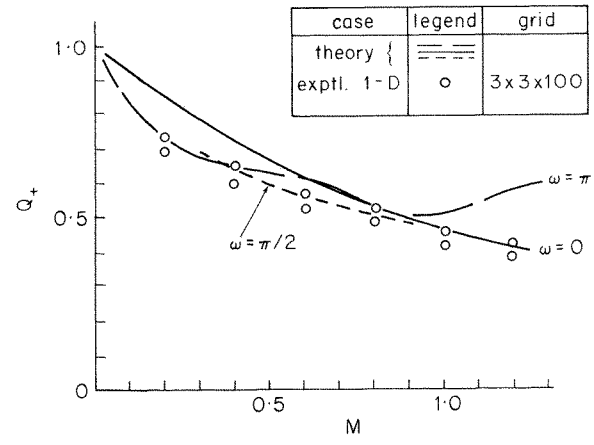

Figure 4. Stability margin Q against Mach number M with perturbation frequency ω for Ahrabian/Denton scheme with time marching using current values of both pressure and density

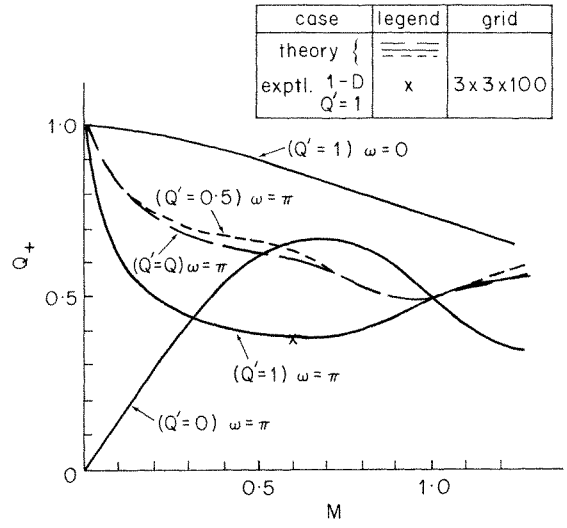

Figure 5. Stability margin Q against Mach number M with perturbation frequency ω for Ahrabian/Denton scheme for various values of Q': $Q'=0$, old level values (OL); $Q'=Q$, time marching (TM); $Q'=1$, conventional damping (CD)

(i.e. $Q'=Q$). The single experimental point found for economy at $M=0{\cdot}6$ in the case of CD indicates that the stability margin is being determined at this Mach number by the frequency $\omega=\pi$. Compared with TM, the CD scheme shows a considerable loss of stability in this case which was tested because at $\omega=0$, the introduction of CD indicates a significant improvement in stability margin. Figures 3, 4 and 5 offer ample confirmation of the validity of the theory.

Figure 6 shows results of using the Highton[3] staggered grid scheme of Figure 2 where all terms in the equations are centrally differenced and used with CD. In this case the reduced,

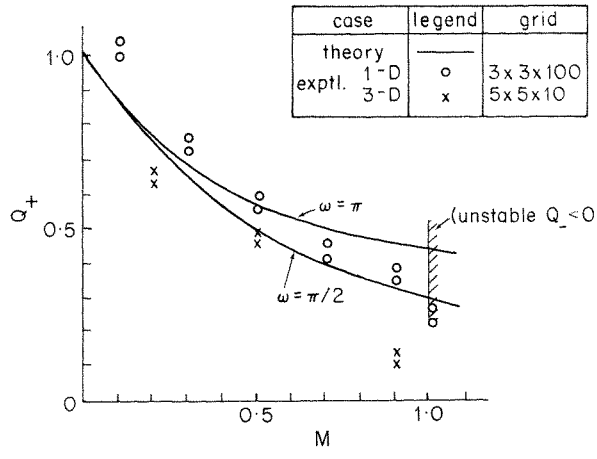

Figure 6. Stability margin Q against Mach number M with perturbation frequency ω for Highton scheme used with centred differencing, current values and conventional damping ($Q=1$), Q_- = value of Q using negative sign

discretized equations read

$$\bar{E}=\frac{1}{c}\begin{bmatrix}\dfrac{2}{\rho_{p-1}+\rho_p}\left\{\rho_p\left(\dfrac{V_p+V_{p+1}}{2}\right)^2-\rho_{p-1}\left(\dfrac{V_{p-1}+V_p}{2}\right)^2+c^2(\rho_p-\rho_{p-1})\right\}\\ \dfrac{\rho_p+\rho_{p+1}}{2}V_p-\dfrac{\rho_{p-1}+\rho_p}{2}V_p\end{bmatrix} \tag{88}$$

which are of second order accuracy. The force term $c^2(\rho_{p-1}-\rho_p)$ is taken at its current value. It should be observed that in this scheme subscript p referring to the nodal point is different for the two variables ρ and V. The Figure shows that this second order scheme has a higher stability margin than the same scheme where the convection of V and ρ are taken upwind, thereby incurring first order error as in References 1 and 3. This scheme has zero quasi-viscosity and serves to reinforce the point,[1] that numerical stability and quasi-viscosity have no direct relationship, but in schemes with first order error, both vanish simultaneously. The stability margin of the experimental results appears to be slightly better than the theory suggests because the number of iterations demanded by the experiments was such that the end boundaries were exercising some stabilizing influence. This point was discussed and illustrated in Reference 1.

COMPARISON OF SCHEMES USING CURRENT VALUES

Reference 1 analysed only OL schemes for which stability vanishes as $M \to 0$. This occurs because in the natural formulation of the equations of motion and continuity (see (86)) the a and d terms of (40) contain M as a factor whereas for stability in subsonic flow the b and c terms are required to be negative conjugate so that λ_{R_n} in (52) vanishes at $M=0$. Since for OL schemes $Q'=0$, then (56) renders $R_c \to \infty$ and these schemes are unstable at this point.

With the use of current values $Q' \neq 0$ so that at $M=0$, by (53), (54) and (55), (56) becomes

$$R_c=\frac{Q}{4Q'}\frac{sqrt[(I_a+I_d)\pm sqrt]^2}{I_bI_c[sqrt\pm(I_a+I_d)]}$$

and since $I_a=0=I_d$

$$R_c=\frac{Q}{Q'} \tag{89}$$

so that for both TM, where $Q'=Q$, $R_c=1$ and for CD, where $Q'=1$, $R_c=Q$ the schemes become stable without modification to the discretization scheme. It can be shown from (49a) that because $a=0=d$ and $bc=-2(1-\cos\omega)$ when $M=0$ for all the schemes based on a natural formulation of the equations as in (86), $Q=1$ at $M=0$ for all ω so that the use of current values transforms loss of stability of OL schemes into the point of maximum stability with a margin of 1. This improved margin is found to continue throughout the subsonic and into the supersonic flow regime.

For TM schemes Figure 7 depicts the stability margin at $\omega=0$ for the Ahrabian scheme, the Highton scheme using upwind convection of V and ρ[3] and the scheme which uses a common upwind operator on all difference terms, which for OL values leads to the Courant–Friedrich–Lewy (CFL) condition[1] and is stable for only supersonic flow. Any of these schemes may be formulated differentially, thus

$$\bar{E}=\begin{bmatrix}\bar{M}\,.\,\text{grad}\,\bar{V}+\dfrac{c}{\rho}\,\text{grad}\,\rho\\ \dfrac{\rho}{c}\,\text{div}\,\bar{V}+\bar{M}\,.\,\text{grad}\,\rho\end{bmatrix} \tag{90}$$

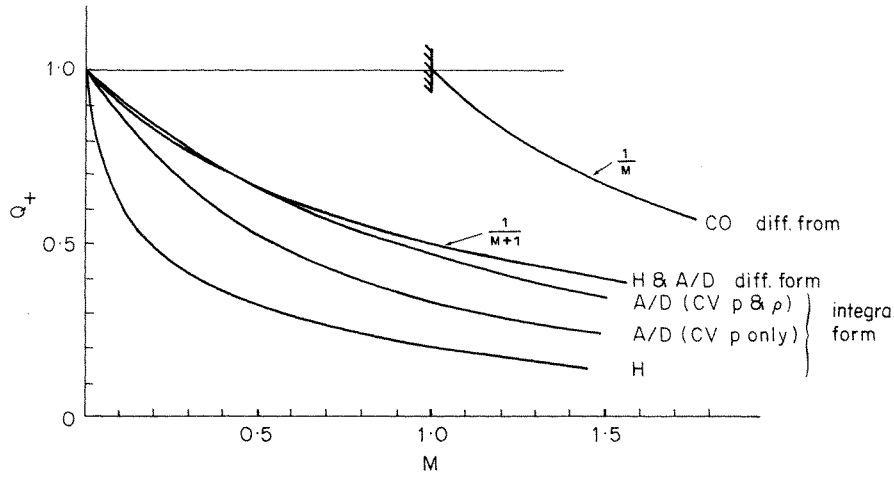

Figure 7. Comparison of stability margin Q against Mach number M at zero perturbation frequency ($\omega = 0$) for various time marching schemes using current values: CO = common operator; A/D = Ahrabian/Denton; H = Highton; CV = current values

or integrally as in (86) and results for both formulations are given in the Figure. The conclusion drawn from these results is that the use of current values shows a universal and greatly improved stability margin to low frequency disturbances at all Mach numbers.

The common upwind operator scheme which is differentially formulated remains stable only for supersonic flow but at $M = 1$ the stability margin is doubled and the CFL condition

$$Q = \frac{1}{M+1} \tag{91a}$$

becomes

$$Q = \left(\frac{1}{M}\right)_{M\leqslant 2}, \qquad Q = \left(\frac{1}{2(M-1)}\right)_{M\geqslant 2} \tag{91b}$$

For the differentially formulated Highton or Ahrabian schemes the stability using the OL scheme,[1] namely

$$Q = \frac{M}{(M+1)^2} \tag{92a}$$

becomes, with the use of current values,

$$Q = \frac{1}{M+1} \tag{92b}$$

i.e. the CFL condition.

As was observed with the OL schemes,[1] differential formulations show a greater stability margin than the corresponding integral formulation.

The integral formulations in Figure 7 all show an improved stability margin at low frequencies when current values are used in place of OL and, although $\omega = 0$ may not in these cases represent the lower bound of Q as may be seen in Figure 4, it has been found in practice that it gives a reasonable guide in the TM schemes and, in these schemes improvements indicated only at $\omega = 0$ have in practice been confirmed by experimental results as general improvements over the full frequency range.

However, for CD schemes it appears that stability with current values is not limited by the low frequency spectrum, which can provide a very misleading impression as shown in Figure 5 where for the Ahrabian scheme the lower bound at $M = 0{\cdot}6$ is close to $\omega = \pi$, stability for $\omega = 0$ being high.

Spalding,[6] employing an integral formulation, uses a staggered grid system which differs from that of Highton in three dimensions but which becomes coincident with it for one dimensional flow. Spalding uses the continuity equation to update the pressure field which, for the isentropic, homentropic flow under consideration, is directly related to the density change thus

$$\mathrm{d}p = c^2 \mathrm{d}\rho \tag{93}$$

However, instead of using the continuity equation as in the natural formulation given in (86) to obtain a density update (via (93)) directly as in (2), he updates the density through a discretized diffusion expression for density change which can be shown to be equivalent here to the formulation

$$\frac{\Delta x}{\rho} \operatorname{div} \operatorname{grad} \rho \delta' \rho = \frac{M}{c} \operatorname{div} (\rho \bar{V}) \tag{94}$$

His momentum equation, which has the same form as that given in (86), may be written

$$\operatorname{div} (\rho \bar{V}) V = -c^2 \operatorname{grad} \rho \tag{95}$$

which is merely a re-arrangement of that in (89). He retains only the nodal terms on the l.h.s. of (5) and (6) and by writing

$$\rho V^2 = \rho^n V^n V^{n+1} \tag{96}$$

obtains equations for ρ^{n+1} and V^{n+1} after suitable division by their factors which are $2A$ for density ρ^{n+1} and $A\rho^n V^n$ for velocity V^{n+1}, the numerical coefficient 2 appearing as a result of the discretization of the diffusive expression div grad.

For this scheme $\bar{E}$ is equivalent to the form

$$\bar{\mathrm{E}} = \begin{bmatrix} \dfrac{1}{\mathrm{M}} \left((\bar{\mathrm{M}} \,.\, \operatorname{grad} + \bar{M} \operatorname{div}) \bar{V} + \dfrac{c}{\rho} (1 + M\bar{M}.) \operatorname{grad} \rho \right\} \\ \dfrac{1}{2} \left\{ \dfrac{\Delta x}{\rho} \operatorname{div} \operatorname{grad} (\rho \delta' \rho) + \dfrac{M}{c} \operatorname{div} (\rho \bar{V}) \right. \end{bmatrix} \tag{97}$$

Spalding uses the continuity equation in an auxiliary cycle, discussed subsequently, in which the density update $\delta\rho$ obtained from $\bar{E}$ is a function of the previous update as can be seen above in (97). This section is concerned only with the stability of the basic cycle consisting of a single pass through the equations of motion and continuity alone and in the absence of an auxiliary cycle which can be introduced into any of the schemes discussed and which is used in the implicit mode of the Highton scheme.[3] Accordingly the diffusive 'pressure' correction term $\dfrac{\Delta x}{\rho} \operatorname{div} \operatorname{grad} (\rho \delta' \rho)$ is omitted in present stability considerations since, as continuity is passed through only once in the cycle, it has no previous correction and is entered with $\delta' \rho = 0$.

Following Spalding's discretization, and re-arranging the equations to read as in (2), they may be written for the present case as

$$\bar{E} = \frac{1}{c}\begin{bmatrix} \frac{c}{V_p}\left\{\left(\frac{2}{\rho_{p-1}+\rho_p}\right)\left\{\rho_p \frac{V_p+V_{p+1}}{2} V_p - \rho_{p-1}\frac{V_{p-1}+V_p}{2} V_{p-1} + c^2(\rho_p - \rho_{p-1})\right\}\right. \\ \left. \frac{1}{2}\left\{\frac{c}{\rho_p}(\rho_{p-1}\delta'\rho_{p-1} - 2\rho_p\delta'\rho_p + \rho_{p+1}\delta'\rho_{p+1}) + \frac{V_p}{c}(\rho_{p+1}V_{p+1} - \rho_p V_p)\right\}\right. \end{bmatrix} \quad (98)$$

where the mass flux in the momentum equation is centred but the velocity convection is upwinded whereas the density convection in continuity is downwinded and the volume flux is centred (as a result of the staggered grid system[1]). It must be observed that in this grid system the nodal points for velocity and density do not coincide. Spalding's momentum equation here differs from Highton's in that it is effectively scaled by $1/M$ (cf. equation (88) where $M = V_p/c$) and his continuity equation differs in two important respects. Because of the formulation based on diffusive correction his continuity equation is effectively scaled by the factor $\frac{1}{2}$, it is further scaled by the factor M and his density convection is downwinded, whereas Highton's is upwinded. The latter feature alone would render Highton's[8] scheme unstable.

It will be seen from Figure 8 that the low frequency stability of (98) which has a lower bound at $M = 0$, is low at low Mach numbers compared with the naturally formulated schemes for which the *lower bound* of $Q = 1$ at $M = 0$, but maintains a very flat response to Mach number. Whereas the naturally formulated schemes remain stable for supersonic and usually for hypersonic flow, the Spalding formulation becomes unstable for $M \geq 0{\cdot}63$. The lack of low frequency stability of this scheme can be seen in Figure 8 to result mainly from the diffusive pressure correction coefficient of $\frac{1}{2}$ which scales the continuity equation, with some further contribution from the downwinded density convection. When an upwinded density convection term and non-diffusive pressure correction are applied the stability margin is improved by some 20 per cent. The limited stability range is marginally improved by the non-diffusive formulation and is completely removed when upwinded density convection is adopted. When both modifications are adopted the low frequency stability margin at

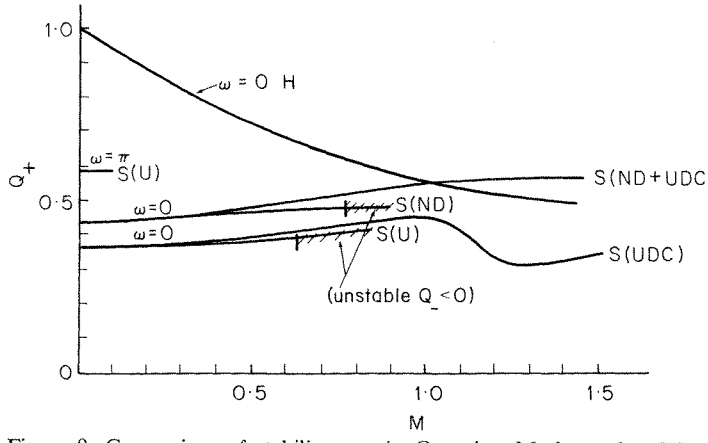

Figure 8. Comparison of stability margin Q against Mach number M at zero perturbation frequency ω for various forms of the Spalding scheme and for the Highton scheme using conventional damping: H = Highton; S = Spalding; ND = non-diffusive pressure correction (i.e. continuity × 2); UDC = Upwind density convection; U = unmodified. Q_- = value of Q using negative sign

$M = 1$ coincides with that of Highton as then the difference is only one of scaling factors $1/M$ and M which are then unity. It is clear that the great loss of stability at low Mach numbers results from these last two factors which arise because of the manner in which the equations are formulated from the steady state equations by the removal of terms to the l.h.s. and subsequent division by factors containing fluid properties.

APPLICATION OF AUXILIARY CYCLE

The effects of introducing an auxiliary cycle in the manner discussed in the latter part of the section 'Use of Auxiliary Cycle' is illustrated here by application to the discretized equations as used by Highton[3] and Splading.[6] The purpose of this illustration is to demonstrate the superior stability, inherent in the type of auxiliary equation which is employed and to show how some composite cycles are improved by its introduction. The auxiliary cycle considered here is of the Highton form and does not take precisely the form employed in the method of Spalding.

The auxiliary equations are constructed by omitting the momentum term from the equation of motion but otherwise retaining the remaining forms of the equations of motion and continuity as used by Highton and Spalding respectively. From (98) these equations read

$$A\delta\bar{x} = \frac{1}{c}\begin{bmatrix} \dfrac{c}{V_p}\left(\dfrac{2}{\rho_{p-1}+\rho_p}\right)\{c^2(\delta\rho_p - \delta\rho_{p-1}\} \\ \dfrac{1}{2}\left\{\dfrac{c}{\rho_p}(\rho_{p-1}\delta\rho_{p-1} - 2\rho_p\delta_p + \rho_{p+1}\delta\rho_{p+1}) \right. \\ \left. + \dfrac{V_p}{c}(\rho_{p+1}\delta V_{p+1} + V_{p+1}\delta\rho_{p+1} - \rho_p\delta V_p - V_p\delta\rho_p)\right\} \end{bmatrix} \tag{99}$$

for the Spalding case which includes the Laplace pressure correction term, and

$$A\delta\bar{x} = \frac{1}{c}\begin{bmatrix} \left(\dfrac{2c}{\rho_{p-1}+\rho_p}\right)c^2(\delta\rho_{p+1} - \delta\rho_p) \\ \dfrac{1}{c}(\rho_p\delta V_p + V_p\delta\rho_p - \rho_{p-1}\delta V_{p-1} - V_{p-1}\delta\rho_{p-1}) \end{bmatrix} \tag{100}$$

for the Highton case. It will be seen from Figure 9 that the stability margin of the Spalding form of auxiliary equation is very high, especially when repeated (i.e. $r > 1$) and considerably improves the margin, as well as extending the Mach number range of the composite cycle into the supersonic regime. The Highton auxiliary cycle is seen in Figure 10 to have a lower stability margin than the Spalding form auxiliary cycle but the composite cycle is shown to gain similarly in stability margin. The range of stability in the Highton case is not limited by either the main cycle or the auxiliary cycle and the greater margin achieved by the composite cycle results from the greater margin of the main cycle. Although the general improvement obtained by the use of the auxiliary cycle is clear, the effect is seen to be heavily weighted by the main cycle margin. The enormous enhancement of stability margin enjoyed by the repeated auxiliary cycle alone is occasioned by the appearance of the quadrature term B^2 in (78).

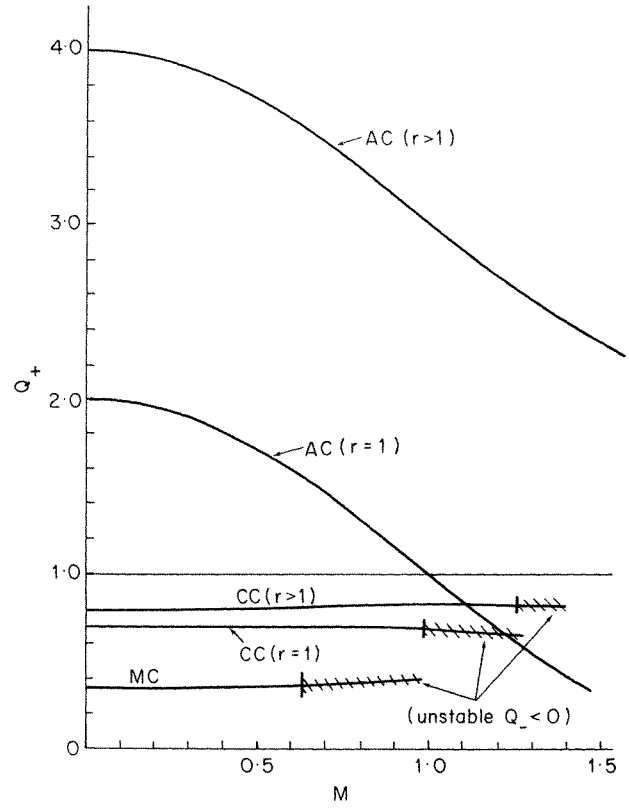

Figure 9. Stability margin Q against Mach number M at zero perturbation frequency ω for Spalding scheme; AC = auxiliary cycle alone; r = number of iterates of AC; CC = composite cycle; MC = main cycle alone. Q_- = value of Q using negative sign

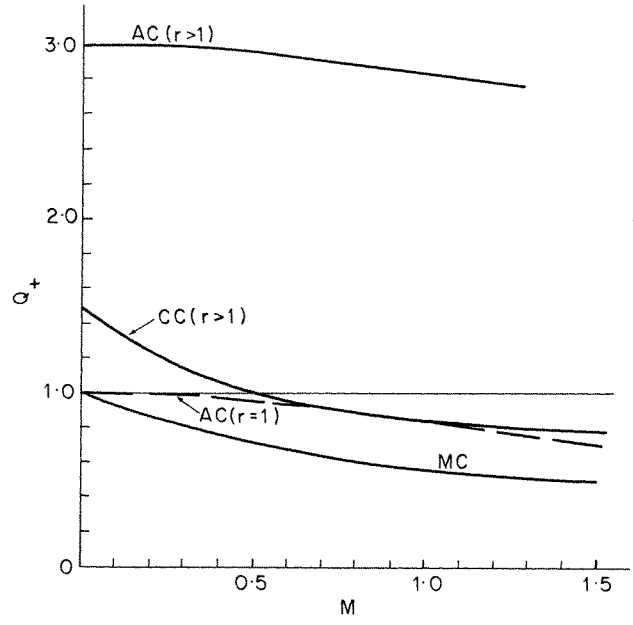

Figure 10. Stability margin Q against Mach number M at zero perturbation frequency ω for Highton scheme: AC = auxiliary cycle alone; r = number of iterates of AC; CC = composite cycle; MC = main cycle. Conventional damping

SCHEMES WITH IMPROVED ACCURACY

The fundamental disadvantage of the schemes so far discussed which rely upon some degree of upwinding to some or all the terms of the equations, lies in the concomitant lack of accuracy incurred for such schemes. The stabilizing upwind device introduces first order truncation error into the discretized equations from which is inferred an increased error in the general solution.

Attempts to reduce this error may be sought by direct reduction of truncation error in the discretization of the terms in the equations or by alternative device which attempt to correct the error as an adjunct to the existing equations by deferred corrections. This section is concerned only with the direct approach first mentioned above.

It is shown in the third section that all formulations of difference expressions which eliminate the first order truncation error, simultaneously reduce the real part α of the Fourier perturbation difference operator (27) to zero, as $\omega \to 0$. This results in the condition (32) which reduces λ_{R_n} in (52) to zero with the consequence that for OL schemes (for which $Q'=0$) R_c in (56) is infinite and the scheme is therefore unstable. For TM schemes (for which $Q'=Q$)

$$R_c = \frac{\lambda_{I_n}^2}{2\lambda_{R_{n+1}}} > 1 \tag{101}$$

if current values are used (see (56)), which is unstable and unaffected by the imposed value of Q in (3). However, for CD schemes using current values (for which $Q'=1$)

$$R_c = \frac{Q\lambda_{I_n}^2}{2\lambda_{R_{n+1}}} \tag{102}$$

which are stabilized by an imposed value of

$$Q < \frac{2\lambda_{R_{n+1}}}{\lambda_{I_n}^2} \tag{103}$$

provided all $\lambda_R > 0$ for $\omega \neq 0$.

Such schemes possess zero quasi-viscosity yet are stable. This stability exists by virtue of $\lambda_{R_{n+1}}$ being a function only of the imaginary part of the difference operators (27) which occurs due to the product $(G_{n+1}G_n)$ in (36) as a result of using current values. Equations (53) and (55) in (103) yield for $\omega \to 0$

$$R_c = \frac{Q}{4I_bI_c}\frac{[sqrt \pm (I_a + I_d)]}{sqrt} \tag{104}$$

$$> 0 \quad \text{(for stability with } Q > 0) \tag{105}$$

hence

$$sqrt > (I_a + I_d)$$

whereby from (54)

$$I_bI_c > I_aI_d \tag{106}$$

For all the integrally formulated schemes, as $\omega \to 0$

$$\begin{aligned} I_bI_c &= (1+M^2) \\ I_aI_d &= 2M^2 \end{aligned} \tag{107}$$

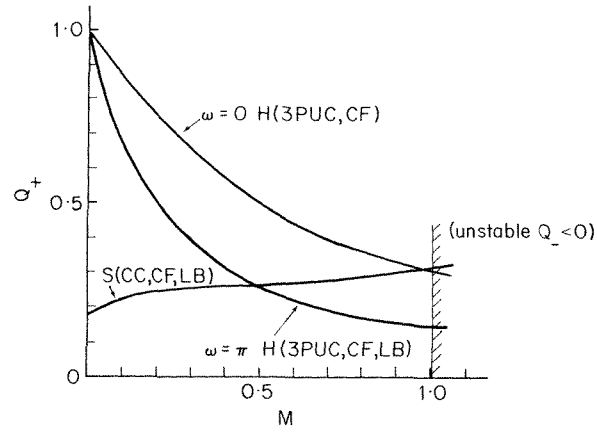

Figure 11. Comparison of stability margin Q against Mach number M for Highton and Spalding schemes with improved accuracy: H = Highton; S = Spalding; CC = centred convection; CF = centred flux; 3PUC = 3 point upwind convection; LB = lower bound. Conventional damping

whereas for the differential schemes

$$I_b I_c = 1$$
$$I_a I_d = M^2 \tag{108}$$

so that in either case (106) becomes

$$1 > M^2 \tag{109}$$

thereby limiting the improved accuracy to subsonic flow on account of the low frequency stability response.

The staggered grid system is the simplest case to improve in the sense that many terms are already automatically centred as a result of the grid system and as these schemes usually use interpolation centred flux terms it is only the convection component of the leading diagonal terms of G which contain first order error. The result of introducing two point centred convection terms into the Highton and Spalding schemes can be seen in Figure 11. These schemes now contain only second order error and the figure shows the lower bound of Q for the main cycle only. Both schemes are stable, the Spalding scheme having suffered a loss of stability margin (cf Figure 8) but a gain in range to $M = 1$. The Highton scheme, surprisingly, but confirmed by experimental results in Figure 6, experiences a considerable gain in stability margin relative to the original TM upwind convection scheme (see Figure 7) which is of first order error.

The Highton scheme has been alternatively improved by using three point upwind biased convection terms in place of the two point centred terms. Figure 11 shows a considerable loss of stability as a result of this upwind bias. This result too must be contrasted with the first order error schemes where upwind bias increases stability margin. The centred convection schemes have a lower bound of Q determined by $\omega \to 0$ at $M = 0$ moving to $\omega = \pi/2$ over most of the range, whereas the upwind biased scheme has a lower bound corresponding to $\omega = \pi$ throughout the range.

The centring of the difference operators renders both real and imaginary parts zero at $\omega = \pi$ so that schemes using a single grid system have a null stability matrix, G, at this frequency and are unstable. The staggered grid system retains its stability because the b and

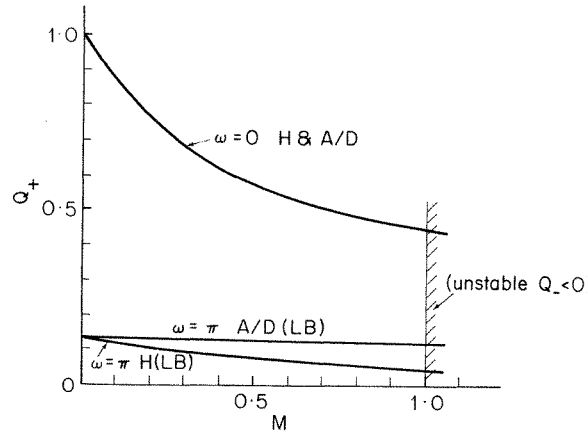

Figure 12. Comparison of stability margin Q against Mach number M for Highton and Ahrabian/Denton schemes modified for improved accuracy: H = Highton with 3PUD on terms a, b, d and 3PDD on term c; A/D = Ahrabian/Denton 3PUD on terms a, c, d and 3PDD on term b; 3PUD = 3 point upwind differencing; 3PDD = 3 point downwind differencing. Conventional damping

c terms of G whilst deriving from centred expressions by virtue of the staggered grid, nevertheless give rise to perturbed difference operators which appear respectively to be upwinded and downwinded. Therefore, whereas the Ahrabian[1] and Denton[2] schemes are not able to take advantage of centred differencing, they do remain stable for three point differencing if the original upwind and downwind bias is retained. Figure 12 shows the stability margin for this case, in which the force term in the equation of motion (i.e. b in G) is downwinded, the remaining terms being upwinded. The lower bound of stability margin governed by $\omega = \pi$ is very low. The figure also shows the lower bound for the Highton scheme in which a similar differencing scheme has been adopted, which renders some terms of third order error. Here again the lower bound is for $\omega = \pi$ and is very low. The stability margin for $\omega = 0$ is common for all naturally formulated schemes in which the first order error has been eliminated and is shown in this Figure.

Within the limitations imposed by the methods so far considered no scheme has been discovered that will extend the higher accuracy stability range to supersonic flow. To acheive this it appears to be necessary to take the diagonal terms a and d of G, over to the l.h.s. of the equations which would involve removing the momentum flux in the equation of motion and the density convection term $\bar{V}$. grad ρ in the continuity equation to the l.h.s. With these modifications the Highton scheme is stable for supersonic flow when used with three point biased differencing.

CONCLUSIONS

In TM formulations the use of current values of the variables as they become available leads to an improved stability margin, most markedly at low Mach numbers. In these formulations the stability appears to be limited by the low frequency perturbations.

Natural formulations (see Introduction) using CD usually show a higher stability margin to low frequency perturbations but their overall stability is usually lower than the corresponding TM case and is determined by other perturbation frequencies.

The introduction of differencing operators which reduce the truncation error in the discretization, simultaneously reduce the stability margin in all cases with the exception of that of Highton when used with CD.

Differential formulations of the equations always offer a larger stability margin than the corresponding integral formulation.

All the schemes analysed retain some margin of stability when improved by reduction of truncation error to the second order. The staggered grid systems remain stable with a good margin when all differencing operators are centred and in the Highton scheme with CD the stability margin is actually improved. Unstaggered grid systems are unstable for centrally differenced operators but retain a low stability margin when three point biased differencing is used. All these schemes are stable only for subsonic flow.

The auxiliary cycles in normal use have very high stability margins and when used with the main equations to form a composite cycle have the effect of improving the stability of the composite cycle.

One-dimensional experiments carried out using three-dimensional computer programs confirm the validity of the one-dimensional Fourier stability analysis. In general it is found experimentally that the stability limit in three dimensions coincides with that in one dimension. The simple analysis is thereby able to indicate which developments will be successful in improving methods of computing three-dimensional, compressible flow. The results of all experiments so far undertaken have validated the theory in relation to predicting whether a scheme will or will not be stable and to predicting the margin of stability.

The mechanism through which individual details of a scheme operate to affect stability can be clearly stated but the relationships involved are generally too complicated to allow directions of development to be drawn from it. However, some broad characteristics relating to stability are evident.

NOMENCLATURE

Latin characters

a, b, c, d	coefficients in equations (5), elements of the governing matrix G (equation (40))
c	speed of sound (equation (8))
e	base of natural logarithms (equation (30))
f	generalized element a, b, c, d (equation (50))
g, h	elements of the matrix $G_{n+1}G_n$ (equations (46) and (48))
i	$\sqrt{-1}$
sqrt	as defined in (54)
t	time
$\bar{x}$	vector of primitive variables
z	space co-ordinate (equation (8))
A	matrix of auxiliary equations, flow area (p. 140)
B	modified auxiliary matrix as defined in equation (68)
$\bar{E}$	the discretized equations of motion
$\bar{E}'$	a subset of E (used in auxiliary cycle)
G	governing stability matrix, G_A corresponding to A, G_B corresponding to B
I	unit matrix
M	Mach number
Q	damping factor, stability margin
Q'	coefficient in equation (49)
R_c	radius of curvature of λ locus at $\omega = 0$ (equation (20))

R_a, R_b, R_c, R_d	real part of differencing operators a, b, c, d (equation (32))
V	fluid velocity

Symbols and greek letters

α, β	coefficient of ω^2 (equations (28) and (31))
$\delta\bar{x}$	as defined in (12)
$\delta\bar{x}'$	as defined in (57)
δ	infinitesimal increment
Δ	finite increment
γ	coefficient in differencing operator (38)
$\sum$	summation (equation (14))
$\bar{\Sigma}$	vector sum (equation (71))
[ ]	vector of variables
[ ]	matrix
[0]	null matrix
:=	becomes
λ	eigenvalue (e.g. λ_G eigenvalue of G)
ω	Fourier frequency parameter
ρ	fluid density
grad	gradient operator
div	divergence operator
$\bar{}$	vector

Subscripts

1, 2	distinct variable as x_1, x_2
j, m, s	grid points other than nodal (equations (28) and (30))
n	as G_n = matrix corresponding to variables $\bar{x}_n$ (equation (10))
p	nodal point
r	as A_r = auxiliary matrix corresponding to variables $\delta'\bar{x}^{n+r}$ (equation (65))
I	imaginary part (coefficient of i) (equation (22)
R	real part (equation (22)

Superscripts

n	iteration number indicating level of variable in main cycle
r	iteration number indicating level of variable in auxiliary cycle
s	solution value (equation (9))

Abbreviations

CD	conventional damping as in (equation (4))
l.h.s.	left hand side of equations
OL	old level values only in the equations $\bar{E}$
r.h.s.	right hand side of equations
TM	time marching as in equation (3)

REFERENCES

1. C. Bosman and D. Ahrabian, 'Numerical stability in three dimensional compressible flow calculations', *J. Heat and Fluid Flow*, **2** (4), 233 (1980).
2. J. D. Denton, 'A time marching method for two and three dimensional blade-to-blade flows', *ARC R & M*, No. 3775, (1975).
3. C. Bosman and J. Highton, 'A calculation procedure for three-dimensional, time-dependent, inviscid, compressible flow through turbomachine blades of any geometry', *JMES* **21** (1), 39 (1979).
4. M. Al-Nakeeb, 'A calculation of steady, inviscid, three-dimensional flow in turbomachines', *Ph.D. Thesis*, Dept. of Mech. Eng., UMIST, 1976.
5. H. Marsh and H. Merryweather, 'The calculation of subsonic and supersonic flows in nozzles', *Symp. on Int. Flows*, Paper 22, Univ. of Salford, 1971.
6. L. S. Caretto, A. D. Gosman, S. V. Patankar and D. B. Spalding, 'Two calculation procedures for steady, three-dimensional flows with recirculation', *Proc. 3rd Int. Conf. Num. Methods in Fluid Mech.*, pp. 66–68, July (1972).
7. C. Bosman and M. J. Hill, 'The effect of damping factor on the behaviour of flow calculations in turbomachines. Pt. 1, *ARC R & M*, No. 3766, (1974).
8. J. Highton, 'The computation of three-dimensional viscous flow with generalised geometry', *Ph.D. Thesis*, Dept. of Mech. Eng., UMIST, 1976.